

CO₂-Uptake Enhances Chromate Release from Fresh Chromium Ore Processing Residues (COPR)

LAPP F.^{1,*}, BRÜCK F.¹, MANSFELDT T.², DOHRMANN R.³, GÖSKE J.⁴ and WEIGAND H.¹

¹Competence Centre for Sustainable Engineering and Environmental Systems (ZEuUS), THM University of Applied Sciences, Wiesenstr. 14, 35390 Gießen, Germany

²Soil Geography/Soil Science, Department of Geosciences, University of Cologne, Albertus-Magnus-Platz, 50923 Cologne, Germany

³Federal Institute for Geosciences and Natural Resources, Stilleweg 2, 30655 Hannover, Germany

⁴ZWL – Zentrum für Werkstoffanalytik Lauf, Hardtstraße 39b, 91207 Lauf a. d. Pegnitz, Germany

*corresponding author:

e-mail: florian.lapp@lse.thm.de

Abstract Chromium ore processing residue (COPR) still contains considerable chromate which can lead to groundwater contamination at uncontrolled dumpsites. The alkaline pH and presence of portlandite introduced in the high-lime roasting render COPR a potential CO₂-trap. To assess whether this feeds back on chromate mobility, fresh COPR samples from two Indian production sites for leather tanning salts were examined. Carbonation was performed at near atmospheric pressure and 100 vol.-% CO₂ for 48 h. The pH, electric conductivity, chromate and bulk anions were determined in aqueous batch leachates of the carbonated and native samples. In addition, the latter were spiked with Na₂CO₃ and titrated with HNO₃ to the pH observed in the carbonated material to distinguish mere pH effects on chromate release from carbonation. The samples sequestered up to 5.0 wt.-% CO₂, decreasing the pH and increasing chromate release by up to 270%. The mobility enhancement was stronger in the carbonated than the pH-adjusted samples. Weathering of COPR and the concomitant uptake of CO₂ may thus increase the risk of groundwater contamination at COPR dumpsites.

Keywords: COPR, Carbonation, Chromate, Leaching

1. Introduction

Chromium Ore Processing Residue (COPR) is a hazardous waste. It is the byproduct of the industrial production of trivalent chromium (Cr(III)) salts (Burke *et al.* 1991). Cr(III) is used for leather tanning, an important industrial branch in the Kanpur region in Uttar Pradesh, India (Tathavadkar *et al.* 2001). COPR still contains high levels of residual Cr(VI) (Geelhoed *et al.* 2002), with chromate (CrO₄²⁻) as the predominant species at alkaline pH (Szabó *et al.* 2018). Leaching of chromate has led to heavy groundwater contamination at uncontrolled dumpsites, which has been extensively described by Matern *et al.* (2017) for the Kanpur region. During the so-called high-lime roasting process, chromite ([Mg,Fe][Cr,Al]₂O₄) is crushed, mixed with limestone (CaO) and soda ash (Na₂CO₃), roasted at roughly 1100 °C and leached with water in a consecutive step (Burke *et al.* 1991). The

remnants of this process are called COPR. The addition of lime and subsequent hydration cause formation of Portlandite, which gives COPR its highly alkaline pH and renders it a potential CO₂-trap as depicted in Figure 1.

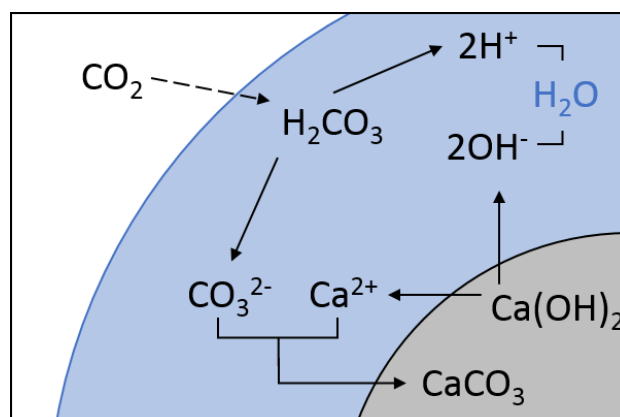


Figure 1. Conceptualization of the carbonation reaction

Little is known about how carbonation impacts chromate mobilization, since most studies examining its weathering have focused on hydration processes (Hillier *et al.* 2003; Boecher *et al.* 2012; Matern *et al.* 2016). We were able to obtain fresh and unweathered COPR samples from two Indian production sites, carbonated them under controlled conditions and analyzed changes in leaching behavior. We compared carbonation-induced effects (namely alkalinity consumption and presence of CO₃²⁻) individually through pH-adjusted and anion-spiked leachates.

2. Material & Methods

2.1. Sampling & Sample Characterization

Sampling for this study was conducted during a field investigation in Uttar Pradesh, India, in 2014. The samples were obtained directly from production sites for leather tanning salts, right after the leaching process, thus representing fresh, unaged COPR. One facility was in

Unnao, north-east of Kanpur, and conducted chromite roasting in batch furnaces, while the other one was in Bindki, south-east of Kanpur, and utilized a rotary kiln. All samples were manually homogenized by intensive stirring with a shovel, air-dried and sieved (Matern *et al.* 2016). The grain size fraction > 2 mm was discarded. Grain size distribution of the fine fraction was determined by dry sieving. Unless otherwise stated, the experiments were conducted using intact material. When needed, aliquots were ground with a stainless-steel ball mill (Pulverisette 6, Fritsch GmbH). Bulk elemental composition of the samples was determined by X-ray Fluorescence (XRF) spectrometry (Axios Fast, Malvern Panalytical GmbH). Total Cr(VI) was quantified with an improved alkaline digestion method specifically adjusted to the analysis of COPR, at (90 ± 10) °C, (48 ± 1) h and employing a liquid/solid ratio (L:S) of 1000 (Mills *et al.* 2017).

2.2 Accelerated Carbonation

To accelerate the natural weathering process under controlled conditions, the samples were exposed to a 100 vol.-% CO₂ atmosphere at near atmospheric pressure for (48 ± 1) h. Tests were conducted in a stainless-steel batch reactor under fixed-bed conditions. The reactor setup was the same as described by Schnabel *et al.* (2021b). The samples were manually hydrated to an L:S of 0.17 and loosely spread on sieve trays contained in a sampling rack. After two purging cycles, the rack was placed inside the air-tight reactor. Gas pressure was monitored in line by two OxiTop-C pressure loggers (Xylem Analytics Germany GmbH). The relative humidity and temperature were logged with an integrated sensor (IP-TH78ext, Arexx Engineering). The gas inlet valve was controlled by the two pressure sensors. The valve was closed when the relative gauge pressure reached (80 ± 10) hPa and was opened when it dropped below (-120 ± 10) hPa upon CO₂-sequestration. From the resulting time-dependent pressure course, the CO₂-uptake ζ_{CO_2} [wt.-%] was calculated according to equation (1):

$$\zeta_{CO_2} = \sum_{i=1}^k \frac{(p_i - p_{i+1}) \cdot V_{Gas}}{R \cdot T} \cdot \frac{M_{CO_2}}{m_{Sample}} \cdot 100 \quad (1)$$

where p_i is the gauge pressure at interval i [hPa], V_{Gas} is the reactor volume minus the rack and sample volumes [m³], R is the ideal gas constant [8.314 J·mol⁻¹·K⁻¹], T is the mean temperature inside the reactor, M_{CO_2} is the molar mass of CO₂ [44 g·mol⁻¹] and m_{Sample} is the hydrated sample mass weighed into the sampling rack. The carbonated samples were dried at 60 °C in a drying chamber.

2.3 Batch Leaching Tests

Aqueous batch leaching tests of the native and carbonated samples were conducted in PE bottles with RO water at an L:S ratio of 10. In two additional batch experiments the native samples were spiked with 1 mol·L⁻¹ of Na₂CO₃ and NaNO₃ in order to assess the effect of anion exchange on the leachability of Cr(VI). Samples were agitated for (24 ± 1) h on an end-over-end shaker (GFL GmbH). Aliquots of the supernatant were passed through 0.45 µm cellulose acetate syringe filters. Electric conductivity (EC) and pH

of the aqueous samples were measured on an Orion VersaStar multimeter (Thermo Scientific Inc.) with potentiometric electrodes. Aqueous Cr(VI) was measured photometrically (Cadas 30 LPG 279, Lange GmbH). The 1,5-Diphenylcarbazide (DPC) standard method according to DIN 38405-52 (2018) has a rather low calibration range of only 0.01 – 1 mg·L⁻¹. Given the fact that aqueous Cr(VI) often exceeded 1000 mg·L⁻¹ we opted for the direct measurement at $\lambda = 374$ nm according to Sanchez-Hachair and Hofmann (2018) with a calibration range of 1 – 24 mg·L⁻¹ and simplified sample preparation. All Cr(VI) measurements were conducted in quadruplicate.

2.4 pH-dependent Leaching

To assess the samples' acid neutralization capacities (ANC) and to study how the carbonation-induced pH drop impacts Cr(VI) mobilization, the native samples were adjusted to defined pH endpoints employing an automated titrator (T70, Mettler Toledo AG). Titrations were carried out with 1 M HNO₃ for 24 h under constant stirring. The initial L:S ratio was 10, ensuring comparability to the batch leachates. Target pH values were 11, 10, 9, 8 and 7 and each titration was conducted in duplicate. HNO₃ was chosen as the titrant since previous tests confirmed that dissolved NO₃⁻ had no significant influence on Cr(VI) mobilization. Filtration and analyses were performed as described above.

3. Results & Discussion

3.1 Bulk Composition of COPR

The samples' elemental composition, given in Table 1, is very similar. The most abundant elements are Ca, Fe, Cr, Mg, Al and Si. This is in line with reports of COPR from Scotland (Geelhoed *et al.* 2002), the US (Boecher *et al.* 2012) and India (Matern *et al.* 2016). The high content in Ca also reflects the high-lime roasting process, where the crushed ore is mixed with limestone. Around 20 % of the total Cr (Unnao) and 23 % (Bindki) were identified as Cr(VI). This, too, is in line with literature data. Matern *et al.* (2016) reported values of 13 – 20 % using standard alkaline digestion, Geelhoed *et al.* (2002) found 30 % using X-Ray Absorption Near Edge Spectroscopy (XANES) and Hillier *et al.* (2003) calculated a fraction of 20 – 25 % from quantitative mineralogical analyses.

Table 1. Bulk elemental composition of the samples

Parameter	Unnao [wt.-%]	Bindki [wt.-%]
Ca	24.9	22.4
Fe	10.5	22.4
Cr	9.1	8.9
Cr(VI)	1.8	2.1
Mg	6.0	5.6
Al	4.6	4.5
Si	2.3	2.2

3.2 CO₂-Sequestration

Fresh COPR is a highly alkaline residue. The native samples' leachate pH values were 11.7 (Unnao) and 12.2

(Bindki), indicating high potential for CO₂-sequestration. Despite that, experimental carbonation has to the best of our knowledge never been tested on COPR. Table 2 gives an overview of the carbonation results. Fast and frequent drops of the reactor pressure indicated high reactivity for both samples. The CO₂-uptake over 48 h amounted to 4.0 (Unnao) and 5.0 (Bindki) wt.-%. Those are remarkable sequestration capacities when compared to other alkaline wastes: In a recent study using the same batch reactor setup, CO₂-uptake over 48 h was 9.5 wt.-% for stainless-steel slag, 5.5 wt.-% for refuse-derived fuel ash, 5.3 wt.-% for biomass bottom ash and 2.6 wt.-% for biomass fly ash (Schnabel *et al.* 2021b). In that setup, however, ideal moisture contents favoring carbonation had been predetermined for each sample, which was not the case for the COPR. Carbonation caused a drop in leachate pH by 2.1 units (final pH = 9.6) for Unnao COPR and by 1.9 units (final pH = 10.3) for Bindki COPR. The latter, despite having sequestered 1 wt.-% of CO₂ more, exhibited a lower pH drop. This may be explained by its much higher buffer capacity. In our 24 h titration tests, the Unnao sample had an acid neutralization capacity at pH 10 (ANC_{pH=10}) of (193 ± 2) mmol_{H+}·kg⁻¹ while it was (585 ± 3) mmol_{H+}·kg⁻¹ for Bindki. This is likely due to their difference in grain size distribution. When both samples were tested after milling, they exhibited roughly similar acid neutralizing behavior (data not shown) which is in line with their similar elemental composition according to XRF.

3.3 Chromate Leaching

The CO₂-uptake also caused a significant increase in leachate Cr(VI) concentration from (375 ± 9) to (552 ± 32) mg·L⁻¹ for Unnao and from (161 ± 2) to (598 ± 59) mg·L⁻¹ for Bindki, which is an increase of roughly 270%. No such obvious effects were observed for other bulk anions (data not shown). To distinguish between the effects of acidification and presence of dissolved CO₃²⁻ on chromate mobilization (both induced by CO₂-sequestration), we performed endpoint titration tests and added Na₂CO₃ to an additional set of batch leachates. Figure 2 shows the result of the endpoint titrations. The release of Cr(VI) was indeed pH dependent, as its concentration increased with decreasing pH and peaked around pH 9. This trend is in line with literature values and is most likely caused by dissolution of Cr(VI) bearing minerals like Cr(VI)-hydrocalumite (Geelhoed *et al.* 2002; Tinjum *et al.* 2008). The decrease in aqueous Cr(VI) below pH 9 is perhaps due to increased chromate adsorption onto Fe-Hydroxides (Tinjum *et al.* 2008). The aforementioned effects were stronger for the Bindki than the Unnao sample. This, too, is most likely due to differences in grain size distribution. Tinjum *et al.* (2008) and Xiao and Li (2012) also

concluded that penetration into the COPR particles was the rate-limiting factor for an acid neutralization.

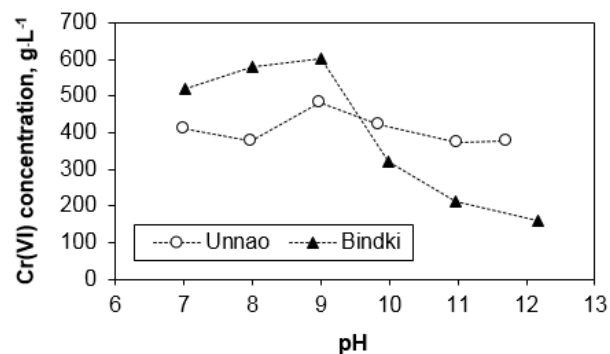


Figure 2. Cr(VI) mobilization through titration with HNO₃

However, titrating the native samples to the pH of the carbonated COPR yielded a significantly lower chromate release. This indicates that the carbonation-enhanced mobility of Cr(VI) cannot be explained by a mere pH effect but may be additionally influenced by the presence of dissolved CO₃²⁻ as a competing anion. Indeed, upon addition of 1 mol·L⁻¹ Na₂CO₃ to the aqueous batch extractions of the native COPR the Cr(VI) concentrations increased from (375 ± 9) to (1023 ± 59) mg·L⁻¹ for Unnao and from (161 ± 2) to (1280 ± 6) for Bindki. This even surpasses the Cr(VI) release caused by the accelerated carbonation. An overview of chromate release caused by the applied leaching methods is given in Figure 3.

4. Conclusion

The results show that weathering of COPR and concomitant CO₂-sequestration by this waste material at uncontrolled dumpsites enhances Cr(VI) leaching and the risk of groundwater contamination.

This knowledge may be useful to improve the leaching process during production of Cr(III) salts or for the development of remediation strategies, which in the past were unable to overcome COPR's slow kinetics of chromate release (Chrysochoou *et al.* 2008). Instead of using acid to liberate chromate, which would require extensive amounts according to ANC values, carbonation could be performed at low cost, e.g. in a rotating drum setup (Schnabel *et al.* 2021a). Ongoing work is directed to a better understanding on how supply of dissolved CO₃²⁻ feeds back on chromate mobility. Layered Double Hydroxides, a mineral class which is frequently identified in COPR and known to potentially hold exchangeable chromate, are of particular interest in this context.

Table 2. CO₂-uptake and subsequent pH drop compared to ANC and grain size distribution

Sample	CO ₂ -Uptake [wt.-%]	pH _{Native}	pH _{Carbonated}	ANC _{pH=10} [mmol _{HNO3} ·kg ⁻¹]	1 – 2 mm grains [wt.-%]	0.1 – 0.25 mm grains [wt.-%]
Unnao	4.0	11.7	9.6	193 ± 2	53.8	13.7
Bindki	5.0	12.2	10.3	585 ± 3	7.3	26.5

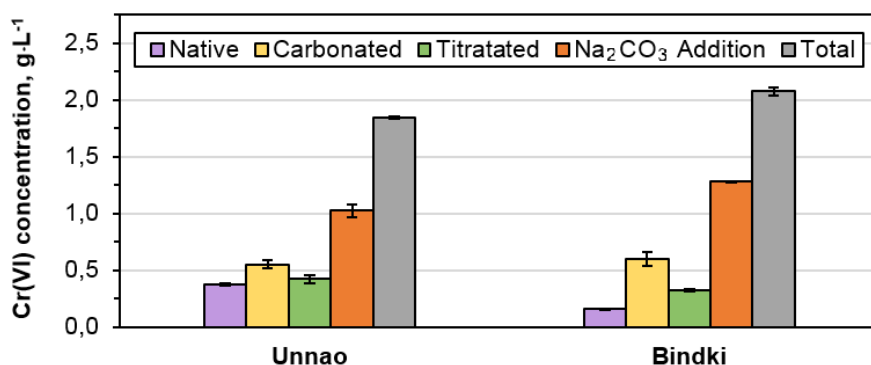


Figure 3. Overview of a aqueous Cr(VI) levels released by different approaches

References

- Boecher T.A., Tinjum J.M., Huifang X. (2012), Quantification of Mineralogical and Amorphous Species in Chromium Ore Processing Residue, *Journal of Residuals Science & Technology*, **9**, 131–141.
- Burke T., Fagliano J., Goldoft M., Hazen R.E., Iglewicz R., McKee T. (1991), Chromite ore processing residue in Hudson County, New Jersey, *Environmental Health Perspectives*, **92**, 131–137.
- Chrysochoou M., Dermatas D., Moon D.H., Christodoulatos C. (2008), Reductive Treatment of Chromite Ore Processing Residue (COPR): Lessons from a Field Study. In *GeoCongress 2008*, Khire, MV, Alshawabkeh, AN, Reddy, KR (eds), American Society of Civil Engineers: Reston, VA, 748–755.
- Deutsches Institut für Normung (2018), *DIN 38405-52: 2018 - Deutsche Einheitsverfahren zur Wasser-, Abwasser- und Schlammuntersuchung - Anionen (Gruppe D) - Teil 52: Photometrische Bestimmung des gelösten Chrom(VI) in Wasser (D 52)*, Beuth Verlag.
- Geelhoed J.S., Meeussen J.C.L., Hillier S., Lumsdon D.G., Thomas R.P., Farmer J.G., Paterson E. (2002) Identification and geochemical modeling of processes controlling leaching of Cr(VI) and other major elements from chromite ore processing residue, *Geochimica et Cosmochimica Acta*, **66**, 3927–3942.
- Hillier S., Roe M.J., Geelhoed J.S., Fraser A.R., Farmer J.G., Paterson E. (2003), Role of quantitative mineralogical analysis in the investigation of sites contaminated by chromite ore processing residue, *The Science of the Total Environment*, **308**, 195–210.
- Matern K., Kletti H., Mansfeldt T. (2016), Chemical and mineralogical characterization of chromite ore processing residue from two recent Indian disposal sites, *Chemosphere*, **155**, 188–195.
- Matern K., Weigand H., Singh A., Mansfeldt T. (2017), Environmental status of groundwater affected by chromite ore processing residue (COPR) dumpsites during pre-monsoon and monsoon seasons, *Environmental Science and Pollution Research*, **24**, 3582–3592.
- Mills C.T., Bern C.R., Wolf R.E., Foster A.L., Morrison J.M., Benzel W.M. (2017), Modifications to EPA Method 3060A to Improve Extraction of Cr(VI) from Chromium Ore Processing Residue-Contaminated Soils, *Environmental Science & Technology*, **51**, 11235–11243.
- Sanchez-Hachair A., Hofmann A. (2018), Hexavalent chromium quantification in solution: Comparing direct UV–visible spectrometry with 1,5-diphenylcarbazide colorimetry, *Comptes Rendus Chimie*, **21**, 890–896.
- Schnabel K., Brück F., Mansfeldt T., Weigand H. (2021a), Full-scale accelerated carbonation of waste incinerator bottom ash under continuous-feed conditions, *Waste Management*, **125**, 40–48.
- Schnabel K., Brück F., Pohl S., Mansfeldt T., Weigand H. (2021b), Technically exploitable mineral carbonation potential of four alkaline waste materials and effects on contaminant mobility, *Greenhouse Gases: Science and Technology*, **3**, 566.
- Szabó M., Kalmár J., Ditrói T., Bellér G., Lente G., Simic N., Fábrián I. (2018), Equilibria and kinetics of chromium(VI) speciation in aqueous solution – A comprehensive study from pH 2 to 11, *Inorganica Chimica Acta*, **472**, 295–301.
- Tathavadkar V.D., Antony M.P., Jha A. (20019), The Soda-Ash Roasting of Chromite Minerals: Kinetics Considerations, *Metallurgical and Materials Transactions B*, **32**, 593–602.
- Tinjum J.M., Benson C.H., Edil T.B. (2008), Mobilization of Cr(VI) from chromite ore processing residue through acid treatment, *The Science of the Total Environment*, **391**, 13–25.
- Xiao K., Li G.C. (2012), Leaching Mechanism of Cr(VI) from Chromite Ore Processing Residue with Nitric Acid, *Advanced Materials Research*, **450-451**, 764–768.